A static voltage stability detector using only local measurements of droop-controlled generators for stressed power distribution networks

Zhao Wang and Michael Lemmon
Department of Electrical Engineering
University of Notre Dame
Notre Dame, IN 46556
Email: zwang6@nd.edu and lemmon@nd.edu

***Abstract*—To assess static voltage stability in power networks, critical load values were examined at each load bus as a voltage instability predictor. However, the information that is required to evaluate loadability conditions is usually not available at load buses. To predict impending voltage collapse in a droop-controlled power distribution network, this paper introduces a static voltage stability detector that only uses local measurements at generator buses. The local stability detector derives a voltage threshold from dynamics of each droop-controlled generator. Monte Carlo simulations are conducted in the IEEE nine-bus network to evaluate the detector's receiver operating characteristic (ROC). Simulations show that the local voltage stability detector has a better performance than loadability conditions in a stressed power distribution network with droop-controlled generators and requires much less information to implement.**

***Index Terms*—Voltage stability, droop-controlled generator, Monte Carlo simulation, receiver operating characteristic.**

I. INTRODUCTION

A power network enters a state of voltage instability when a change in system condition causes an uncontrollable voltage drop [1]. Voltage instability is mainly caused by the power system's inability to supply enough reactive power, such as in a stressed power network. There is a growing concern about stressed power networks due to increasing electricity demand and aging infrastructure. Furthermore, power distribution networks will operate closer to their voltage stability limits as distributed energy resources (DERs) are present. Since power networks become vulnerable to voltage collapse, power system operators need to detect impending voltage instability effectively.

Similar to power system transient stability analyses, voltage stability conditions were derived using Lyapunov-based methods [2]. However, distribution system operators prefer an indicator showing how close a system is to voltage collapse, such as a critical load impedance for each load bus. These loadability conditions were derived using either model-based methods or measurement-based methods. In model-based methods, a *Thevenin* equivalent circuit was obtained based on local measurements at each load bus [3][4], reflecting the network's relative strength. Nevertheless, it may not be possible to collect measurements and compute an equivalent circuit model at every load bus. In addition, because various physical constraints were included, model-based methods were too complex for real-time applications. To obtain voltage stability margins in real-time, measurement-based methods were proposed that required a power network's global phase angle information from phasor measurement units (PMUs) [5][6]. Along this direction, a wide-area voltage stability monitoring system [7] was developed that measured and communicated relative phase angles throughout power networks. Load buses, however, do not install PMUs in many power distribution networks. As a result, neither approach analyzed static voltage stability without requiring information from *every* load bus.

To solve these problems, a local voltage stability detector is proposed for stressed power distribution networks with droop-controlled generators. Unlike PMU-based monitoring systems in [6][7], the detector only examines local states at each generator bus and computes a voltage threshold. This voltage stability detector is tested in the IEEE nine-bus network. Monte Carlo simulations are conducted to evaluate the detector's receiver operating characteristic (ROC) that plots detection probability versus false-alarm rate. The local voltage stability detector performs better than loadability conditions in [3][4] and requires much less information.

The remainder of this paper is organized as follows. Section II introduces notations used in this paper. Section III describes a stressed network model with droop-controlled rotational and electronic generators. Section IV presents the voltage stability detector that only uses local measurements of generator buses. Section V demonstrates simulation results showing that the voltage stability detector performs better in predicting impending voltage collapses than loadability conditions. Section VI provides concluding remarks of this voltage stability detector.

II. NOTATIONS

This section introduces notations used in static voltage stability analyses. Three-phase balanced operation and per-unit (p.u.) normalization are basic assumptions. Under these assumptions, admittance matrix $\boldsymbol{Y}_{n\times n}$ of an n-bus network is defined as a symmetric complex matrix [8], which does not include shunt admittances. Admittance matrix $\boldsymbol{Y}_{n\times n}$ is also expressed as $\boldsymbol{Y}_{n\times n} = \boldsymbol{G}_{n\times n} + j\boldsymbol{B}_{n\times n}$, where $\boldsymbol{G}_{n\times n}$ is conductance matrix and $\boldsymbol{B}_{n\times n}$ is susceptance matrix.

The authors gratefully acknowledge the partial financial support of Notre Dames Environmental Change Initiative and the National Science Foundation (CNS-1239222).

978-1-4673-8040-9/15/$31.00 ©2015 IEEE

A generator and a load connect to each bus: $P_{gen,i}$ and $Q_{gen,i}$ are generated power; $P_{load,i}$ and $Q_{load,i}$ are real and reactive loads. At any bus i, E_i is voltage magnitude and δ_i is phase angle; P_i and Q_i are injected power. Power flows at bus i are $P_i = P_{gen,i} - P_{load,i}$ and $Q_i = Q_{gen,i} - Q_{load,i}$. A pure load bus j has $P_j + P_{load,j} = 0$ and $Q_j + Q_{load,j} = 0$. Power injections P_i and Q_i at bus i are expressed in *power balance* relationships

$$P_i = \sum_{j=1, j\neq i}^{n} E_i E_j |Y_{ij}| \sin(\delta_i - \delta_j + \phi_{ij}) - E_i^2 |Y_{ij}| \sin \phi_{ij},$$

$$Q_i = \sum_{j=1, j\neq i}^{n} E_i^2 |Y_{ij}| \cos \phi_{ij} - E_i E_j |Y_{ij}| \cos(\delta_i - \delta_j + \phi_{ij}),$$

where $\phi_{ij} = \phi_{ji} = \tan^{-1}(\frac{G_{ij}}{B_{ij}}) \in [-\frac{\pi}{2}, 0]$.

Stressed power networks arise when electricity demand increases and infrastructure ages. Stressed network scenarios also emerge from connecting DERs to transfer large power flows through long feeders [9]. Power flow stress is quantified using a short-circuit ratio (SCR) [9] as a ratio between the short circuit power at a generator bus and this generator's maximum apparent power, for instance, the nine-bus network in Section V is under stress with its SCR below 30.

A power distribution network includes various types of loads that are represented using a ZIP load model [10]. ZIP model is a polynomial load model that combines constant-impedance (Z), constant-current (I) and constant-power (P) components. Real and reactive loads at bus i are defined as functions of voltage magnitude E_i (in p.u.) as

$$P_{load,i} = E_i^2 P_{load,a,i} + E_i P_{load,b,i} + P_{load,c,i},$$
$$Q_{load,i} = E_i^2 Q_{load,a,i} + E_i Q_{load,b,i} + Q_{load,c,i},$$

where $P_{load,a,i}$ and $Q_{load,a,i}$ are nominal constant-impedance loads, including shunt devices; $P_{load,b,i}$ and $Q_{load,b,i}$ are nominal constant-current loads, denoting devices that are modeled as current sources; $P_{load,c,i}$ and $Q_{load,c,i}$ are nominal constant-power loads, generally as a result of power control mechanisms. As a result, this ZIP model represents a variety of loads and control devices.

III. System Model

In this paper, an n-bus power distribution network is modeled with m electronic generator buses, g rotational generator buses, and l load buses. *Assumption* 1 and 2 are made about this n-bus power network.

Assumption 1: Each generator bus connects to the power distribution network through a load bus.

Assumption 2: Load increase is considered as the disturbance that causes voltage instability situations.

Electronic generators are managed by a droop controller, for instance, using the CERTS (Consortium for Electric Reliability Technology Solutions) droop-control mechanism [11]. For m electronic generator buses, voltage dynamic equation of the ith electronic generator is

$$\dot{E}_i = (E_{ref,i} - E_i) - m_{Q,i} Q^m_{gen,i}, \tag{1}$$

for all $i \in \{1, 2, \ldots, m\}$, where $m_{Q,i}$ is droop slope of the Q-E droop controller. In equation (1), $E_{ref,i}$ denotes voltage control command; $Q^m_{gen,i}$ is measured power as a feedback to the Q-E droop controller. Slope of the droop controller, i.e. $m_{Q,i}$, also reflect the reactive power capacity of the electronic generator at bus i. For g rotational generator buses, voltages are assumed to be managed by excitation systems that use droop controllers with dynamics in equation (1).

Low-pass filters (LPFs) represent power measurement dynamics in droop controllers of electronic generators, whose expressions are

$$\tau_{S,i} \dot{Q}^m_{gen,i}(t) + Q^m_{gen,i}(t) = Q_{gen,i}(t), \tag{2}$$

where $\tau_{S,i}$ is power measurement time costant, such as 0.01 *sec* in a CERTS droop controller.

These LPFs affect voltage dynamics. In voltage dynamics, including LPFs leads to $\tau_{S,i}\ddot{E}_i(t) + (\tau_{S,i} + 1)\dot{E}_i(t) + E_i(t) = E_{ref,i} - m_{Q,i} Q_{gen,i}(t)$. When time constant $\tau_{S,i}$ is small, such as 0.01 *sec*, the second-order equation simplifies to

$$\dot{E}_i(t) = (E_{ref,i} - E_i(t)) - m_{Q,i} Q_{gen,i}(t). \tag{3}$$

Equation (3) is similar to equation (1) but ignores power measurement dynamics. Voltage dynamics in equation (3) is used for a power distribution network with droop-controlled rotational and electronic generators.

In the n-bus power network, phase angles of the first $(n-1)$ buses refer to bus n. With phase angle difference $\theta_i = \delta_i - \delta_n$ for all $i \in \{1, 2, \ldots, n-1\}$ and $\theta_n = 0$, a steady state $(\boldsymbol{P}_{ss}, \boldsymbol{Q}_{ss}, \boldsymbol{\theta}_{ss}, \boldsymbol{E}_{ss}, \omega_{ss})$ is a zero point of dynamics in equation (3). To define a power network model, we introduce set point $(\boldsymbol{P}_{set}, \boldsymbol{Q}_{set}, \boldsymbol{\theta}_{set}, \boldsymbol{E}_{set}, \omega_{set})$, which is a steady state. *Assumption* 3 is made for the set point:

Assumption 3: Set point $(\boldsymbol{P}_{set}, \boldsymbol{Q}_{set}, \boldsymbol{\theta}_{set}, \boldsymbol{E}_{set}, \omega_{set})$ is assumed to be an isolated equilibrium point.

Power system operators usually determine a set point by solving an optimal power flow (OPF) problem and designate control command $E_{ref,i}$ to generator bus i as

$$E_{ref,i} = E_{set,i} + m_{Q,i}(Q_{set,i} + Q_{load,i}(E_{set,i})), \tag{4}$$

With respect to set point $(\boldsymbol{P}_{set}, \boldsymbol{Q}_{set}, \boldsymbol{\theta}_{set}, \boldsymbol{E}_{set}, \omega_{set})$, we define a power network model to study voltage stability. Error states are defined with respect to the isolated set point for phase angle $\tilde{\theta}_i = \theta_i - \theta_{set,i}$, voltage magnitude $\tilde{E}_i = E_i - E_{set,i}$ and reactive power $\tilde{Q}_i = Q_{set,i} - Q_i$. Voltage-error dynamics are as follows,

$$\begin{aligned}\dot{\tilde{E}}_i &= (E_{set,i} - E_i) + m_{Q,i}(Q_{gen,set,i} - Q_{gen,i}), \\ &= m_{Q,i}\tilde{Q}_i - \tilde{E}_i - m_{Q,i}[Q_{load,b,i} + (E_i + \tilde{E}_i)Q_{load,a,i}]\tilde{E}_i, \\ &\quad i \in \{1, \ldots, m+g\}\end{aligned} \tag{5}$$

$$\begin{aligned}\tilde{Q}_i &= Q_{load,a,i}\tilde{E}_i^2 + (2Q_{load,a,i}E_{set,i} + Q_{load,b,i})\tilde{E}_i. \\ &\quad i \in \{m+g+1, \ldots, m+g+l\}\end{aligned} \tag{6}$$

Equation (6) shows an algebraic relation between voltage magnitude error $\tilde{E}_i$ and reactive power error $\tilde{Q}_i$ at load buses. Because voltage dynamics are governed by equation (5), voltage stability conditions are derived at generator buses.

IV. Main Result

This section establishes a static voltage stability detector based on local measurements at generator buses. From voltage dynamics of each droop-controlled generator, a voltage threshold is derived that indicates static voltage stability. If voltage at any generator bus i falls below the threshold as load increases, the voltage stability detector initiates a warning.

The following theorem derives a voltage threshold $E_{th,i}$ for each generator bus that characterizes its voltage stability using local measurements.

Theorem 1: For generator bus i and its connected load bus j through a transformer, define parameters with respect to set point $(\boldsymbol{P}_{set}, \boldsymbol{Q}_{set}, \boldsymbol{\theta}_{set}, \boldsymbol{E}_{set}, \omega_{set})$ as $a_i = \frac{Q_{load,a,i}}{|Y_{ij}|} + \cos\phi_{ij}$, $b_i = \frac{\frac{1}{m_{Q,i}}+Q_{load,b,i}+2Q_{load,a,i}E_{set,i}}{|Y_{ij}|} + (2E_{set,i} - E_j)\cos\phi_{ij}$, and $c_i = E_{set,i}E_{set,j}\sin(\theta_i - \theta_j + \phi_{ij})(\tilde{\theta}_i - \tilde{\theta}_j) - E_{set,i}\tilde{E}_j\cos\phi_{ij}$. If these parameters satisfy

$$a_i > 0, \quad b_i > 0, \quad \text{and} \quad c_i > 0, \tag{7}$$

$$b_i^2 - 4a_ic_i > 0, \tag{8}$$

there is a threshold for each generator bus $i \in \{1, \ldots, m+g\}$

$$E_{th,i} = E_{set,i} + \frac{-b_i + \sqrt{b_i^2 - 4a_ic_i}}{2a_i}.$$

If steady state voltage $E_i \le E_{th,i}$ at any generator bus i, the power network enters a state of voltage instability.

Proof: When load increases in a power distribution network, E_i decreases at each generator bus i. Based on equation (5), voltage dynamics at bus i are as follows

$$\frac{\dot{\tilde{E}}_i}{m_{Q,i}} = \tilde{Q}_i - Q_{load,a,i}\tilde{E}_i{}^2 - (1/m_{Q,i} + Q_{load,b,i} + 2Q_{load,a,i}E_{set,i})\tilde{E}_i.$$

For the transformer between generator bus i and load bus j with $\phi_{ij} = 0$, $\tilde{Q}_i$ is bounded from below as

$$\frac{\tilde{Q}_i}{|Y_{ij}|} \ge -\tilde{E}_i^2\cos\phi_{ij} - (2E_{set,i} - E_j)\tilde{E}_i\cos\phi_{ij} - E_{set,i}[E_{set,j}\sin(\theta_i - \theta_j + \phi_{ij})(\tilde{\theta}_i - \tilde{\theta}_j) - \tilde{E}_j\cos\phi_{ij}].$$

Detailed proof of this lower bound is provided in the Appendix. Using the lower bound of $\tilde{Q}_i$, there exists an inequality

$$\frac{\dot{\tilde{E}}_i}{m_{Q,i}} \ge -|Y_{ij}|(a_i\tilde{E}_i^2 + b_i\tilde{E}_i + c_i). \tag{9}$$

If conditions in equations (7) and (8) are satisfied, algebraic equation $a_i\tilde{E}_i^2 + b_i\tilde{E}_i + c_i = 0$ has two negative solutions. When $\tilde{E}_i \in \boldsymbol{T}$ with set $\boldsymbol{T}$ defined as

$$\boldsymbol{T} = \{\tilde{E}_i \in \boldsymbol{R} | \frac{-b_i - \sqrt{b_i^2 - 4a_ic_i}}{2a_i} \le \tilde{E}_i \le \frac{-b_i + \sqrt{b_i^2 - 4a_ic_i}}{2a_i}\},$$

there is $\dot{\tilde{E}}_i > 0$ in set $\boldsymbol{T}$. Obviously, voltage error $\tilde{E}_i$ at any generator bus i does not stay in this set $\boldsymbol{T}$.

As load incrementally increases, the power system is assumed to reach a steady state $E_{ss,i} \le E_{th,i}$. This steady state corresponds to an equilibrium point of voltage error $\tilde{E}_{ss,i} = E_{ss,i} - E_{set,i}$, where $\tilde{E}_{ss,i} \in \boldsymbol{T}$. Define a function $V_{\tilde{E}_i} = \frac{(\tilde{E}_i - \tilde{E}_{ss,i})^2}{2m_{Q,i}}$, which is positive in set $\boldsymbol{U}$ with

$$\boldsymbol{U} = \{\tilde{E}_i \in \boldsymbol{R} | \tilde{E}_{ss,i} < \tilde{E}_i < E_{th,i} - E_{set,i}\}.$$

Since $\boldsymbol{U} \subset \boldsymbol{T}$, derivative of $V_{\tilde{E}_i}$ is also positive in set $\boldsymbol{U}$, as

$$\dot{V}_{\tilde{E}_i} = \frac{(\tilde{E}_i - \tilde{E}_{ss,i})\dot{\tilde{E}}_i}{m_{Q,i}} > 0.$$

According to *Theorem* 4.3 in [12], the equilibrium point $\tilde{E}_{ss,i}$ is not stable. As a result, threshold $E_{th,i}$ is an indication of voltage instability, which is evaluated only based on local measurements at each generator bus. If voltage magnitude E_i at any generator bus i falls below $E_{th,i}$, the power network enters a state of voltage instability. ■

Remark 1: Information used to evaluate $E_{th,i}$ is available or can be computed from measurements at generator bus i.

V. Simulation Experiments

The local voltage stability detector is examined in the IEEE nine-bus simulation model in Figure 1. Compared to loadability conditions, simulation shows that the local voltage stability detector has a better performance and requires much less information to implement.

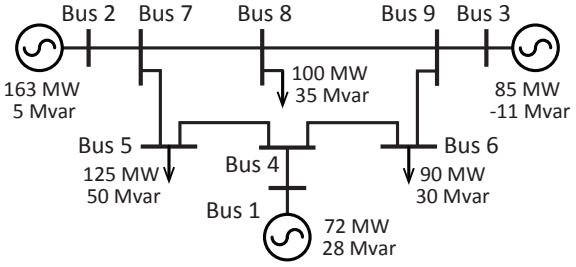

Fig. 1. Modified IEEE nine-bus network with droop-controlled generators (at the original set point)

This network contains three generator buses, three load buses and three connection buses, a total of nine buses. Different from the model in [13], parameters of droop-controlled generators are shown in Table I. Bus 2 and 3 connect to electronic generators that have small inertia M. Each generator also has its real and reactive power generation limits. Two set points are simulated: one set point has original load values in Figure 1, with its SCR below 30; the other set point has 25 MW more real power loads at bus 6 and bus 8 respectively.

At the beginning of each simulation, one of the three load buses is picked at random whose load level increases to a uniformly distributed peak value and then recovers to the original value in a linear fashion. As load level incrementally increases, both voltages and frequencies deviate from the original set point, which may cause voltage instability.

An example of voltage instability is shown in Figure 2. In this example, the load level at bus 5 increases between $t = 1$

TABLE I
DROOP-CONTROLLED GENERATOR PARAMETERS

#	m_Q $p.u.$	M $\frac{MJ \cdot s}{MVA \cdot rad}$	D $\frac{rad/s}{MVA}$	ω_0 rad/s	$[\underline{P}, \overline{P}]$ 100MW	$[\underline{Q}, \overline{Q}]$ 100Mvar
1	0.05	0.0507	0.1959	120π	[0.6,1.37]	[-2.0,2.0]
2	0.033	0.0032	0.3138	120π	[1.0,2.0]	[-3.0,3.0]
3	0.05	0.0023	0.2315	120π	[0.7,1.4]	[-2.0,2.0]

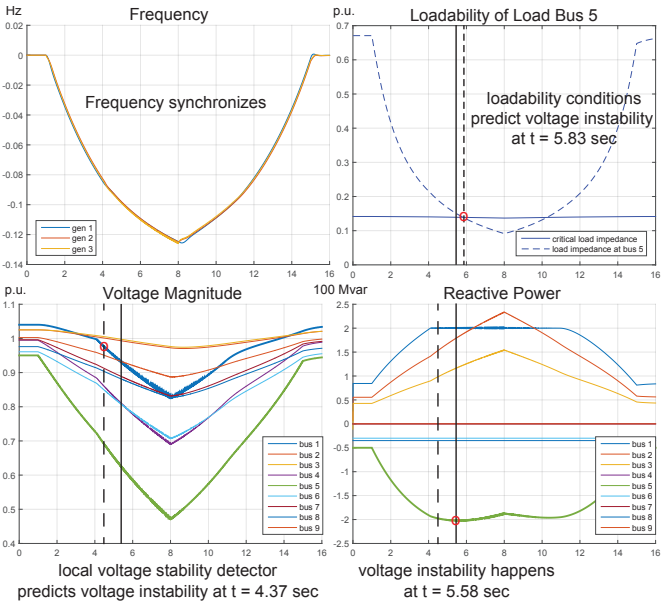

Fig. 2. Example of voltage instability with load increase at bus 5; our voltage stability detector (dashed line in lower plots) predicts impending voltage instability (solid line) while loadability conditions (dashed line in upper right plot) fail.

sec and $t = 8$ sec that causes voltage drops at all buses, as shown in the lower left plot of Figure 2. In the lower right plot, voltage instability happens at $t = 5.58$ sec (solid line) when voltage at load bus 5 decreases but its reactive power consumption reduces, as defined in [1]. The local voltage stability detector predicts voltage instability at $t = 4.37$ sec (dashed line) when voltage E_1 at generator bus 1 reduces below $E_{th,1}$. Loadability conditions, however, detects that load impedance at load bus 5 reaches its critical load impedance at $t = 5.83$, *after* the state of voltage instability begins. This example shows that the local voltage stability detector predicts impending voltage instability while loadability conditions fail.

Monte Carlo simulations are conducted to obtain an ROC curve for loadability conditions and the local voltage stability detector. To plot such a curve, adjustments are made to the threshold $E_{th,i}$ and the critical load impedance. 1500 simulations are conducted using each threshold value to determine a pair of false-alarm rate and detection probability that corresponds to a point. Connecting multiple points, an ROC curve is plotted individually for the local voltage stability detector and loadability conditions, as shown in Figure 3.

At both set points, the local voltage stability detector renders an ROC curve in solid line, while loadability conditions lead to dashed line. With threshold adjustments, the local voltage

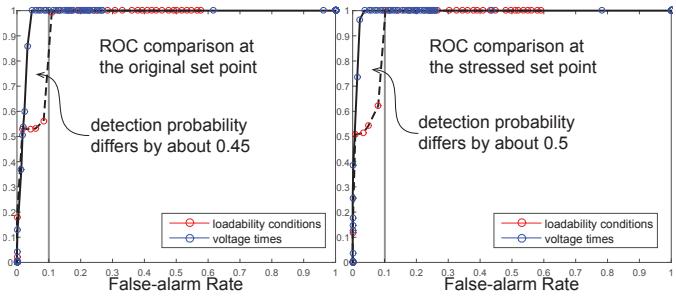

Fig. 3. ROC curves at (left) original set point; (right) stressed set point

stability detector performs better than loadability conditions when false alarm rate is low. At a false alarm rate below 0.1, the local voltage stability detector has a detection probability about 0.45 larger than loadability conditions.

As a result, using voltage thresholds derived in *Theorem* 1, impending voltage collapse is predicted timely. Even with adjustments, the local voltage stability detector performs much better than loadability conditions when false alarm rate is below 0.1. Moreover, the static voltage stability detector only uses local measurements at generator buses, unlike loadability conditions that also require information from all load buses.

VI. CONCLUSION

A static voltage stability detector is derived based on local measurements at each generator bus. If any generator voltage falls below the derived threshold, the power network enters a state of voltage instability. The local voltage stability detector predicts impending voltage instability accurately, while loadability conditions fail. With different adjustments to thresholds, ROC curve of the local voltage stability detector is always above the ROC curve of loadability conditions. As a result, the local voltage stability detector performs better than loadability conditions in predicting voltage instability and requires much less information to implement.

In this paper, our voltage stability is only tested for two set points in a simple nine-bus network so that more work needs to be done. In our future work, we will investigate voltage instability situations that include not only voltage collapse but also over-voltage, as mentioned in [14]. Similar to the lower bound that is used to derive a threshold $E_{th,i}$, an upper bound can be derived that leads to another threshold voltage larger than $E_{set,i}$. After considering both voltage collapse and over-voltage instability, we plan to apply the voltage stability detector to a practical large scale system, such as the IEEE Reliability Test System in [15] or the IEEE 118-Bus standard network. Using these realistic simulation models, performance of our voltage stability detector would be compared to other well-known technologies, such as the method of continuation power flow [16]. The ROC curve of continuation power flow will be compared with the ROC curve of our voltage stability detector, similar to the comparison shown in Figure 3. Moreover, the amount of information that is required to implement each method will be compared.

REFERENCES

[1] P. Kundur, *Power system stability and control*. Tata McGraw-Hill Education, 1994.

[2] P.-A. Lof, G. Andersson, and D. Hill, "Voltage stability indices for stressed power systems," *Power Systems, IEEE Transactions on*, vol. 8, no. 1, pp. 326–335, 1993.

[3] K. Vu, M. M. Begovic, D. Novosel, and M. M. Saha, "Use of local measurements to estimate voltage-stability margin," *Power Systems, IEEE Transactions on*, vol. 14, no. 3, pp. 1029–1035, 1999.

[4] A. Wiszniewski, "New criteria of voltage stability margin for the purpose of load shedding," *Power Delivery, IEEE Transactions on*, vol. 22, no. 3, pp. 1367–1371, 2007.

[5] B. Milosevic and M. Begovic, "Voltage-stability protection and control using a wide-area network of phasor measurements," *Power Systems, IEEE Transactions on*, vol. 18, no. 1, pp. 121–127, 2003.

[6] R. Sodhi, S. Srivastava, and S. Singh, "A simple scheme for wide area detection of impending voltage instability," *Smart Grid, IEEE Transactions on*, vol. 3, no. 2, pp. 818–827, 2012.

[7] J.-H. Liu and C.-C. Chu, "Wide-area measurement-based voltage stability indicators by modified coupled single-port models," 2014.

[8] A. R. Bergen, *Power Systems Analysis, 2/E*. Pearson Education, 2009.

[9] N. P. Strachan and D. Jovcic, "Stability of a variable-speed permanent magnet wind generator with weak ac grids," *Power Delivery, IEEE Transactions on*, vol. 25, no. 4, pp. 2779–2788, 2010.

[10] "Load representation for dynamic performance analysis," *Power Systems, IEEE Transactions on*, vol. 8, no. 2, pp. 472–482, 1993.

[11] R. Lasseter, "Smart distribution: Coupled microgrids," *Proceedings of the IEEE*, vol. 99, no. 6, pp. 1074–1082, 2011.

[12] H. K. Khalil, *Nonlinear systems*. Prentice hall Upper Saddle River, 2002, vol. 3.

[13] A.-H. Amer, "Voltage collapse prediction for interconnected power systems," Ph.D. dissertation, West Virginia University, 2000.

[14] T. Van Cutsem and R. Mailhot, "Validation of a fast voltage stability analysis method on the hydro-quebec system," *Power Systems, IEEE Transactions on*, vol. 12, no. 1, pp. 282–292, 1997.

[15] C. Grigg, P. Wong, P. Albrecht, R. Allan, M. Bhavaraju, R. Billinton, Q. Chen, C. Fong, S. Haddad, S. Kuruganty *et al.*, "The ieee reliability test system-1996. a report prepared by the reliability test system task force of the application of probability methods subcommittee," *Power Systems, IEEE Transactions on*, vol. 14, no. 3, pp. 1010–1020, 1999.

[16] V. Ajjarapu, *Computational techniques for voltage stability assessment and control*. Springer Science & Business Media, 2007.

APPENDIX

In the Appendix, we provide the proof of the lower bound of $\tilde{Q}_i$. Combined with the expression of $\tilde{E}_i/m_{Q,i}$, we obtain equation (9).

Proposition 2: Assume a generator bus i that is connected to load bus j through a transformer with $\phi_{ij} = 0$, $\tilde{Q}_i$ is bounded from below as

$$\frac{\tilde{Q}_i}{|Y_{ij}|} \geq -\tilde{E}_i^2 \cos\phi_{ij} - (2E_{set,i} - E_j)\tilde{E}_i \cos\phi_{ij} - E_{set,i}[E_{set,j} \sin(\theta_i - \theta_j + \phi_{ij})(\tilde{\theta}_i - \tilde{\theta}_j) - \tilde{E}_j \cos\phi_{ij}],$$

which is a second-order polynomial of voltage error $\tilde{E}_i$ at generator bus i.

Proof: Using power balance relationship, relative power error $\tilde{Q}_i$ at generator bus i is expressed as follows

$$\begin{aligned}
\tilde{Q}_i &= E_{set,i}^2|Y_{ij}|\cos\phi_{ij} \\
&\quad -E_{set,i}E_{set,j}|Y_{ij}|\cos(\theta_{set,i} - \theta_{set,j} + \phi_{ij}) \\
&\quad -E_i^2|Y_{ij}|\cos\phi_{ij} + E_iE_j|Y_{ij}|\cos(\theta_i - \theta_j + \phi_{ij}), \\
&= -\tilde{E}_i^2|Y_{ij}|\cos\phi_{ij} - 2E_{set,i}\tilde{E}_i|Y_{ij}|\cos\phi_{ij} \\
&\quad -E_{set,i}E_{set,j}|Y_{ij}|\cos[(\theta_i - \theta_j + \phi_{ij}) - (\tilde{\theta}_i - \tilde{\theta}_j)] \\
&\quad +(E_{set,i} + \tilde{E}_i)(E_{set,j} + \tilde{E}_j)|Y_{ij}|\cos(\theta_i - \theta_j + \phi_{ij}), \\
&= -\tilde{E}_i^2|Y_{ij}|\cos\phi_{ij} - 2E_{set,i}\tilde{E}_i|Y_{ij}|\cos\phi_{ij} \\
&\quad +(\tilde{E}_iE_j + E_{set,i}\tilde{E}_j)|Y_{ij}|\cos(\theta_i - \theta_j + \phi_{ij}) \\
&\quad +E_{set,i}E_{set,j}|Y_{ij}|\cos(\theta_i - \theta_j + \phi_{ij})(1 - \cos(\tilde{\theta}_i - \tilde{\theta}_j)) \\
&\quad -E_{set,i}E_{set,j}|Y_{ij}|\sin(\theta_i - \theta_j + \phi_{ij})\sin(\tilde{\theta}_i - \tilde{\theta}_j).
\end{aligned}$$

The following inequalities are used to derive a lower bound:

- Since $-1 \leq \cos(\tilde{\theta}_i - \tilde{\theta}_j) \leq 1$ for any power flow situation, there is $1 - \cos(\tilde{\theta}_i - \tilde{\theta}_j) \geq 0$;
- Because generator bus i injects power to load bus j through a transformer, phase angles satisfy $\theta_i - \theta_j < 0$ that leads to $\cos(\theta_i - \theta_j + \phi_{ij}) \leq \cos\phi_{ij}$;
- As load increases, power injection from generator bus i rises so that there is a larger phase angle difference between bus i and bus j, i.e. $0 \leq \tilde{\theta}_i - \tilde{\theta}_j \leq \pi/2$ with $\sin(\tilde{\theta}_i - \tilde{\theta}_j) \leq \tilde{\theta}_i - \tilde{\theta}_j$;
- As load increases, voltage errors at both bus i and j are less than zero, i.e. $\tilde{E}_i < 0$ and $\tilde{E}_j < 0$.

As a result, the expression $\tilde{Q}_i/|Y_{ij}|$ is bounded from below as

$$\begin{aligned}
\frac{\tilde{Q}_i}{|Y_{ij}|} &\geq E_{set,i}\tilde{E}_j\cos\phi_{ij} + \tilde{E}_iE_j\cos\phi_{ij} - 2E_{set,i}\tilde{E}_i\cos\phi_{ij} \\
&\quad - \tilde{E}_i^2\cos\phi_{ij} - E_{set,i}E_{set,j}\sin(\theta_i - \theta_j + \phi_{ij})(\tilde{\theta}_i - \tilde{\theta}_j), \\
&= -\tilde{E}_i^2\cos\phi_{ij} - (2E_{set,i} - E_j)\tilde{E}_i\cos\phi_{ij} \\
&\quad - E_{set,i}[E_{set,j}\sin(\theta_i - \theta_j + \phi_{ij})(\tilde{\theta}_i - \tilde{\theta}_j) - \tilde{E}_j\cos\phi_{ij}].
\end{aligned}$$

This is a second-order polynomial of voltage error $\tilde{E}_i$ at generator bus i. Together with expressions of droop controller and ZIP load, voltage stability threshold $E_{th,i}$ is derived for generator bus i. ■

For the case of over-voltage instability, an upper bound can be derived for $\tilde{Q}_i$. Derivation of this upper bound is very similar to deriving the lower bound, with assumptions of positive voltage error $\tilde{E}_i$ and reduced power injection from generator bus i.